Surface Displacement and Ground Motion from Dynamic Rupture Models of Thrust Faults with Variable Dip Angles and Burial Depths

Sirena Ulloa, Julian C. Lozos

California State University, Northridge

Award # 18218

Introduction

Historic earthquakes and empirical studies show that thrust fault ruptures produce stronger ground motion than normal or strike-slip events of the same size due to a combination of hanging wall effects, vertical asymmetry, and higher stress drop resulting from compression. There have been many studies on thrust faults, but most are empirical or lab simulated. Our 3D dynamic rupture modeling parameter study focuses on planar thrust faults of varying dip angles and burial depth, in order to establish a physics-based understanding of how these geometrical parameters affect surface displacement and ground motion. We vary dip angle and burial depth in order to show systematic changes that result from fault geometry—a major driving force in thrust fault ruptures. Our models can help fill gaps in observational studies for different thrust fault geometries, and provide a starting point for understanding hazard for generalized or specific thrust faults.

Physical and Computational Parameters	
Shear Stress	11.25 MPa
Normal Stress	31.25 MPa
Coefficient of Static Friction	0.6
Coefficient of Dynamic Friction	0.2
Critical Slip Weakening Distance	0.4 m
P-wave Velocity	6000 m/s
S-wave Velocity	3464 m/s
density	2700 kg/m^3
element size (fault and surrounding media)	200 m
element size (buffer zone)	600 m
forced nucleation zone radius	3000 m

Methods

We created 36 meshes of planar faults in a homogeneous, elastic half space using Cubit. The mesh is composed of tetrahedral elements, to conform to the geometry of dipping faults. We then used FaultMod (Barall, 2009) to rupture each fault under slip-weakening friction at a nucleation point 3 km updip and from its left edge. Each fault is 30 x 15 km, with a fault strength S of 1.5 and a stress drop $\Delta\sigma$ of 10 MPa. We begin our study with homogeneous initial stresses acting on the fault plane. We also implemented a stress gradient for our tapered stress case, so that initial shear and normal stresses acting on the fault are higher when deeper in the subsurface, since tapering the initial stresses can generate results more fitting to real- world faults, since stress increases deeper in the earth. We tapered the stresses by setting initial stresses to be equal to twice the stresses of the homogenous stress case at the depth of our lowest fault base, then tapered the stresses to 0 at the free surface, and equal to those of our homogenous case at the middle depth.

Basic Fault Geometry

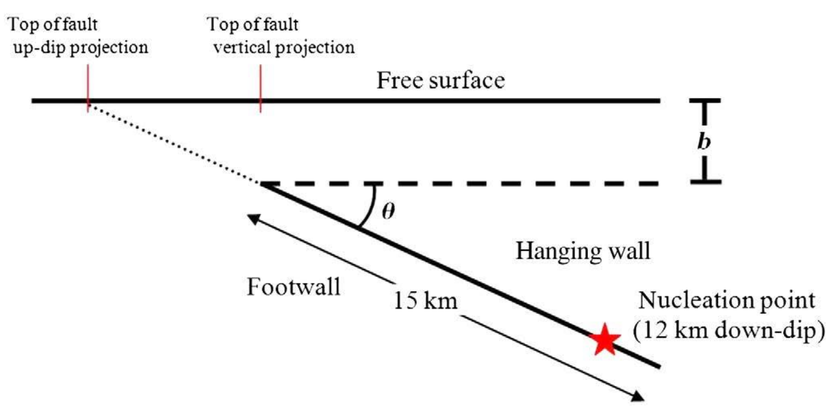

This is the basic setup of each fault in this parameter study.

Varied Dip Angles within Stress Gradient

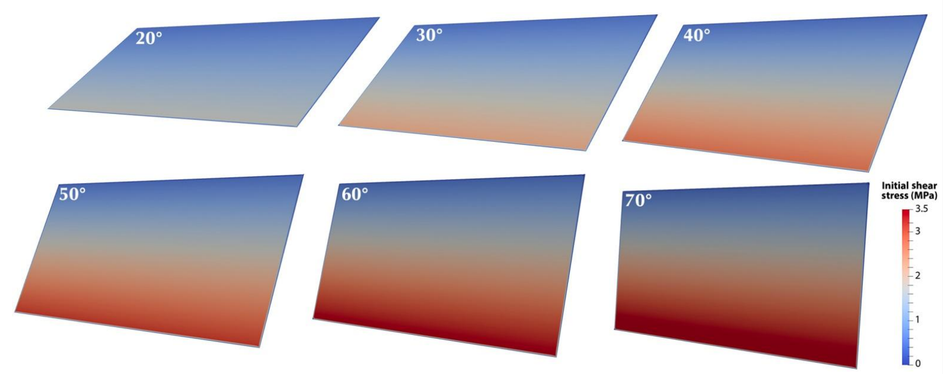

As the dip angle steepens, initial stresses are higher at the base of the fault due to fault geometry.

Horizontal Ground Motion Homogeneous Stress

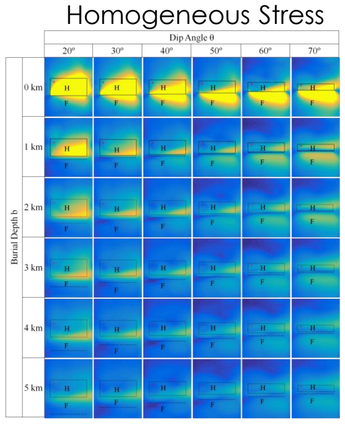

Spatial distribution is prominent at the surface and decreases overall as we bury the fault deeper.

Vertical Ground Motion Homogeneous Stress

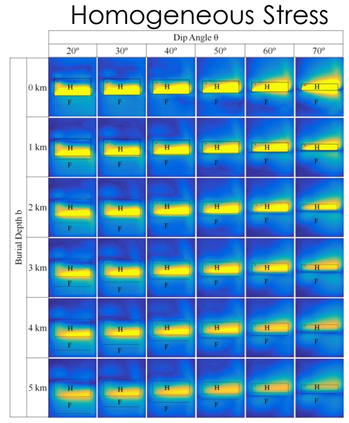

Spatial distribution shifts slightly from hanging wall to footwall with steeper dip angle and decreases as we bury the fault deeper.

Surface Displacement Homogeneous Stress

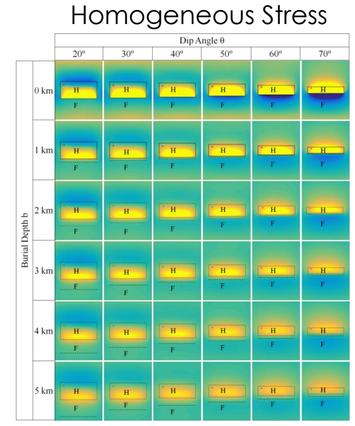

There is more uplift and subsidence resulting from ruptures of shallower depth. More uplift is concentrated on the hanging wall in steeper faults.

Panels:

Map view of thrust faults while varying burial depth and dip angle. Each black box represents the area directly above the fault plane, while the dotted line is the updip projection of a blind thrust fault at the surface, and the red star is the nucleation point (key below).

Horizontal Ground Motion Tapered Stress

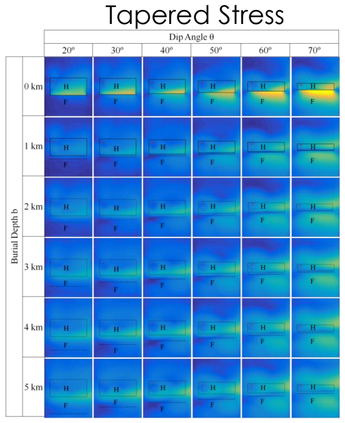

As we steepen the dip angle, there is an increase in ground motion as distribution shifts to the footwall. Strong shaking is prominent in emergent faults.

Vertical Ground Motion Tapered Stress

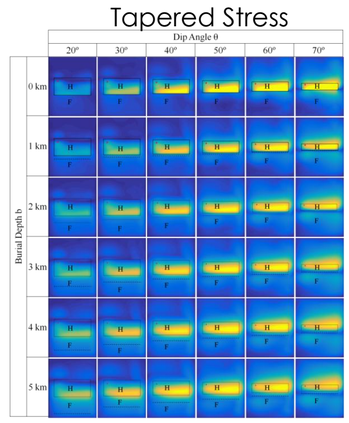

Ground motion is higher in deeper faults and in those with steeper dip angle. Faults with steeper dip angle have more ground motion on the footwall than other faults.

Surface Displacement Tapered Stress

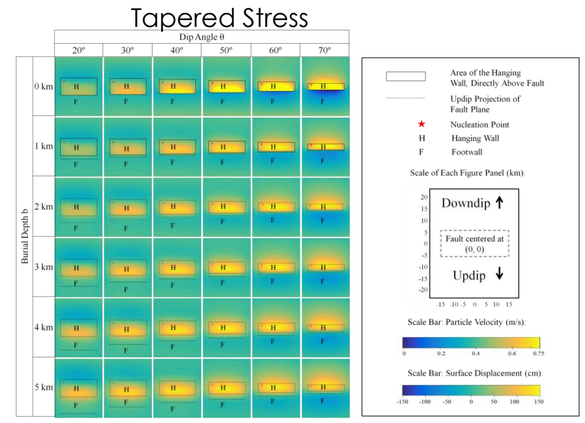

Distributions of uplift and subsidence are similar to homogenous case, but increase with deeper burial depth and steeper dip angle.

Discussion

In our homogeneous case, as we bury faults deeper and steepen dip angle, we see decreased ground motion and surface displacement. This is because wave attenuation and geometric spreading decrease particle velocity in ruptures that nucleate deeper in the subsurface. The area of the surface above the hanging wall is larger in more shallow- dipping faults, and these ruptures nucleate closer to the surface. Moreover, since our homogenous stress models have the same slip regardless of fault geometry, those with steeper dip angles have more uplift than more shallow-dipping faults, since the motion in these cases is closer to pure vertical. Although we were consistent in fault dimension to eliminate magnitude as a factor, we do see slight variations based on the uniformity of initial stresses, and whether the fault is blind or emergent. The highest slip distribution is in the emergent homogeneous stress case, due to a higher energy budget toward the top of the fault, as we are not tapering the initial stresses, and there is no overburden. We do see highest particle velocity in this case, especially for horizontal ground motion. We also see effects on ground motion and surface displacement due to wave amplification. Both ground motion and surface displacement are larger in models of faults with surface expression than in any of the blind thrust cases, and steadily increase with steeper dip angle. However, adding a stress gradient results in less overall variation across different geometries for both particle velocity and surface displacement, when compared to the homogeneous stress case. In our tapered stress case, stress drop is lower near the surface, while ruptures that nucleate deeper in the subsurface begin with higher stress drop. There is a balance between high energy release in deeper ruptures and energy loss due to geometric spreading and wave attenuation. In the case of both homogeneous and tapered initial stresses, uplift and peak vertical ground motions correlate, as they are both controlled by fault geometry and stress drop.

Conclusion

Fault geometry and stress drop systematically drive the variations in ground motion and surface displacement from model to model. Given the geometric simplicity of our models, and that we varied both dip angle and burial depth of thrust faults, and have compared these systematic variations against those with tapered initial stresses, others can apply these results to site-specific studies. Our spatial distribution plots can also help to improve on GMPEs, and aid in geotechnical engineering and hazard science, as we can see variability of particle velocities and surface displacements due to thrust fault ruptures over a parameter space, and this can fill gaps in observational data.

References

Barall, Michael (2009). A grid-doubling finite-element technique for calculating dynamic three-dimensional spontaneous rupture on an earthquake fault, *Geophys. J. Int.* (2009) 178, 845–859 doi: 10.1111/j.1365-246X.2009.04190.x GJI Seismology

Contact: sirena.ulloa.250@my.csun.edu